PERGAMON

International Journal of Solids and Structures 38 (2001) 2271–2290

INTERNATIONAL JOURNAL OF SOLIDS and STRUCTURES

www.elsevier.com/locate/ijsolstr

Non-stationary vibration of multilayer plates of an uncanonical form. The elastic immersion method

A.N. Shupikov *, N.V. Smetankina

Institute for Problems in Machinery, National Academy of Sciences of Ukraine, 2/10 Pozharsky Street, Kharkov 61046, Ukraine

Received 6 February 1999; in revised form 2 December 1999

Abstract

This paper presents an approach to research of vibration of multilayer plates of complicated form under impulse loading. The approach is based on the elastic immersion method. The dynamic behaviour of plates is described within the framework of the theory accounting for transverse shear strains. The boundary conditions for multilayer plates with a curvilinear boundary are obtained. Numerical examples demonstrate functionality of the method offered.

Keywords: Multilayer plates; Uncanonical form; Vibration

1. Introduction

The finite element method (Zienkiewicz, 1971; Segerlind, 1976; Reddy, 1997) and the boundary element method (Banerjee and Batterfield, 1981; Brebbia et al., 1984; Rashed, 1998) are applied primarily for analysis of strain-stressed state of plates of an arbitrary plan form.

Jaswon and Maiti (1968) were the first to apply the boundary element method to the plate-bending problem. In solving such problems the Green functions are generally unknown. Altiero and Sikarskie (1978) have offered an approach when the real plate is embedded into a fictitious round clamped plate for which the Green functions are known.

Further, Zielinski (1980, 1985) used a Kirchoff rectangular simply supported plate as an enveloping plate for studying the plate-bending problem. The technique of expansion of sought-for functions into trigonometrical series was applied for solving the integral equation system instead of a discretization of the given plate boundary.

As noted in the work of Rashed (1998), the majority of known publications deals with static bending problems of plates considered within the framework of the classical theory. The present paper offers the elastic immersion method generalizing the approaches described above to the case of non-stationary deformation of multilayer plates of an uncanonical plan form.

* Corresponding author. Fax: +380-0572-944-635.
E-mail address: kantor@ipmach.kharkov.ua (A.N. Shupikov).

0020-7683/01/$ - see front matter
PII: S0020-7683(00)00166-9

2. Multilayer plate

2.1. Basic relationships

The multilayer plate is assembled from I layers of constant thickness and is referred to the Cartesian coordinate system connected to the outside surface of the first layer (Fig. 1). In the coordinate plane $x0y$ the plate occupies a simply connected domain Ω having a boundary L of an arbitrary form

$$L\colon x_L = x(\varphi), \quad y_L = y(\varphi), \quad \varphi_0 \leqslant \varphi \leqslant \varphi_1. \tag{1}$$

We shall designate the normal and tangent to the boundary L as **n** and **s**, respectively.

The plate is subjected to an external impulse load $\mathbf{P}^{\mathrm{e}} = \{p_j^{\mathrm{e}}(x,y,t)\}$ $(j = \overline{1,2I+3})$ distributed on domain $\Omega_p \subset \Omega$; t being time. The load vector components have the form

$$p_1^{\mathrm{e}} = p_2^{\mathrm{e}} = p_{3+i}^{\mathrm{e}} = p_{3+I+i}^{\mathrm{e}} = 0, \quad p_3^{\mathrm{e}} = p_3^{\mathrm{e}}(x,y,t), \quad x,y \in \Omega_p. \tag{2}$$

The layer strains are described within the framework of the refined theory of plates (Smetankina et al., 1995; Shupikov et al., 1996). The contact between layers excludes their delamination and mutual slipping. The broken line hypothesis holds true for a pack of layers. Displacements of a point in the ith layer have the form

$$\begin{aligned} u^i &= u + \sum_{j=1}^{i-1} h_j \psi_x^j + (z - \delta_{i-1})\psi_x^i, \\ v^i &= v + \sum_{j=1}^{i-1} h_j \psi_y^j + (z - \delta_{i-1})\psi_y^i, \\ w^i &= w, \end{aligned} \tag{3}$$

where

$$\delta_i = \sum_{j=1}^{i} h_j, \quad \delta_{i-1} \leqslant z \leqslant \delta_i, \quad i = \overline{1,I}.$$

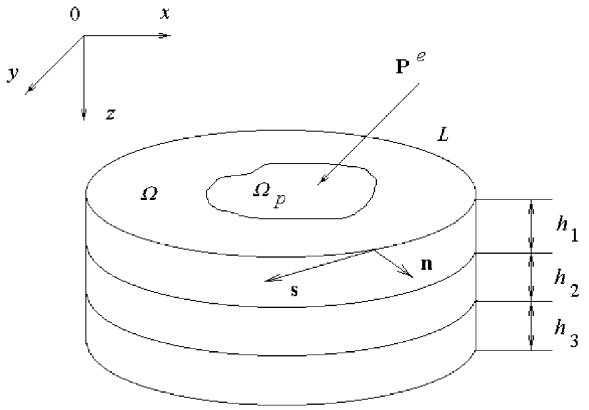

Fig. 1. Multilayer plate.

$u = u(x,y,t)$, $v = v(x,y,t)$, $w = w(x,y,t)$ are displacements of the coordinate plane point in the direction of the coordinate axes; $\psi_x^i = \psi_x^i(x,y,t)$, $\psi_y^i = \psi_y^i(x,y,t)$ are the angles of rotation of a normal element in the ith layer around axes $0x$ and $0y$; h_i is thickness of the ith layer.

The strains of the layers are defined according to Cauchy's formulas

$$\begin{aligned}
\varepsilon_x^i &= u_{,x} + \sum_{j=1}^{i-1} h_j \psi_{x,x}^j + (z - \delta_{i-1})\psi_{x,x}^i, \\
\varepsilon_y^i &= v_{,y} + \sum_{j=1}^{i-1} h_j \psi_{y,y}^j + (z - \delta_{i-1})\psi_{y,y}^i, \\
\gamma_{xy}^i &= \gamma_{yx}^i = u_{,y} + v_{,x} + \sum_{j=1}^{i-1} h_j \left(\psi_{x,y}^j + \psi_{y,x}^j\right) + (z - \delta_{i-1})\left(\psi_{x,y}^i + \psi_{y,x}^i\right), \\
\gamma_{xz}^i &= \gamma_{zx}^i = \psi_x^i + w_{,x}, \gamma_{yz}^i = \gamma_{zy}^i = \psi_y^i + w_{,y}, \quad i = \overline{1,I}.
\end{aligned} \tag{4}$$

Hereafter the expressions $u_{,x}$, $v_{,y}$, etc. denote partial derivatives of the displacements with respect to an appropriate coordinate.

Hooke's law connects stresses and strains in the ith layer

$$\begin{aligned}
\sigma_x^i &= \frac{E_i}{1 - \nu_i^2}\left(\varepsilon_x^i + \nu_i \varepsilon_y^i\right), \qquad \sigma_y^i = \frac{E_i}{1 - \nu_i^2}\left(\varepsilon_y^i + \nu_i \varepsilon_x^i\right), \\
\tau_{xy}^i &= \tau_{yx}^i = \frac{E_i}{2(1 + \nu_i)}\gamma_{xy}^i, \qquad \tau_{xz}^i = \tau_{zx}^i = \frac{E_i}{2(1 + \nu_i)}\gamma_{xz}^i, \\
\tau_{yz}^i &= \tau_{zy}^i = \frac{E_i}{2(1 + \nu_i)}\gamma_{yz}^i, \quad i = \overline{1,I},
\end{aligned} \tag{5}$$

where E_i is Young's modulus, ν_i is Poisson's ratio of the ith layer.

The stress resultants in the ith layer are determined under the following formulas:

$$\begin{aligned}
N_x^i &= \int_{\delta_{i-1}}^{\delta_i} \sigma_x^i \, \mathrm{d}z, \qquad N_y^i = \int_{\delta_{i-1}}^{\delta_i} \sigma_y^i \, \mathrm{d}z, \qquad N_{xy}^i = N_{yx}^i = \int_{\delta_{i-1}}^{\delta_i} \tau_{xy}^i \, \mathrm{d}z, \\
M_x^i &= \int_{\delta_{i-1}}^{\delta_i} \sigma_x^i (\mathrm{z} - \delta_{i-1}) \, \mathrm{d}z, \qquad M_y^i = \int_{\delta_{i-1}}^{\delta_i} \sigma_y^i (\mathrm{z} - \delta_{i-1}) \, \mathrm{d}z, \\
M_{xy}^i &= M_{yx}^i = \int_{\delta_{i-1}}^{\delta_i} \tau_{xy}^i (\mathrm{z} - \delta_{i-1}) \, \mathrm{d}z, \\
Q_x^i &= \int_{\delta_{i-1}}^{\delta_i} \tau_{xz}^i \, \mathrm{d}z, \qquad Q_y^i = \int_{\delta_{i-1}}^{\delta_i} \tau_{yz}^i \, \mathrm{d}z, \quad i = \overline{1,I}.
\end{aligned} \tag{6}$$

2.2. Equations of motion and boundary conditions

Applying Hamilton's variational principle, using Eqs. (3)–(6) and performing appropriate integration by parts, we obtain the equations of motion of a multilayer plate

$$
\begin{aligned}
&\sum_{i=1}^{I}\left(N^i_{x,x}+N^i_{yx,y}\right)+p^{\mathrm{e}}_1=0,\quad \sum_{i=1}^{I}\left(N^i_{xy,x}+N^i_{y,y}\right)+p^{\mathrm{e}}_2=0,\\
&\sum_{i=1}^{I}\left(Q^i_{x,x}+Q^i_{y,y}-\alpha^i_\rho w_{,tt}\right)+p^{\mathrm{e}}_3=0,\\
&h_i\sum_{j=i}^{I-1}\left(N^{j+1}_{x,x}+N^{j+1}_{yx,y}\right)+M^i_{x,x}+M^i_{yx,y}-Q^i_x+p^{\mathrm{e}}_{3+i}=0,\\
&h_i\sum_{j=i}^{I-1}\left(N^{j+1}_{xy,x}+N^{j+1}_{y,y}\right)+M^i_{xy,y}+M^i_{y,y}-Q^i_y+p^{\mathrm{e}}_{3+I+i}=0,\quad i=\overline{1,I},\quad x,y\in\Omega,
\end{aligned}
\tag{7}
$$

where

$$\alpha^i_\rho=\rho_i h_i,\quad i=\overline{1,I},$$

ρ_i being the density of the ith layer material.

Also, the corresponding boundary conditions on boundary L are obtained

$$
\begin{aligned}
&\varsigma_{11}N_n+\varsigma_{12}u_n=0,\qquad \varsigma_{21}N_s+\varsigma_{22}u_s=0,\\
&\varsigma_{31}Q_n+\varsigma_{32}w=0,\qquad \varsigma_{3+i,1}M^i_n+\varsigma_{3+i,2}\psi^i_n=0,\\
&\varsigma_{3+I+i,1}M^i_s+\varsigma_{3+I+i,2}\psi^i_s=0,\quad i=\overline{1,I},\quad x,y\in L,
\end{aligned}
\tag{8}
$$

where u_n, u_s are displacements of a contour point of the coordinate plane in the direction of normal and tangent to the boundary L, respectively; ψ^i_n, ψ^i_s are the angles of rotation of a normal element in the ith layer around the tangent and normal to boundary L, respectively;

$$
\begin{aligned}
&u_n=un_x+vn_y,\qquad u_s=-un_y+vn_x,\\
&\psi^i_n=\psi^i_x n_x+\psi^i_y n_y,\qquad \psi^i_s=-\psi^i_x n_y+\psi^i_y n_x,\quad i=\overline{1,I},
\end{aligned}
$$

N_n, N_s and Q_n are normal tensile, tangential and transverse forces, respectively (Fig. 2a),

$$
\begin{aligned}
&N_n=\sum_{i=1}^{I}N^i_n,\quad N_s=\sum_{i=1}^{I}N^i_s,\quad Q_n=\sum_{i=1}^{I}Q^i_n,\\
&N^i_n=N^i_x n_x^2+N^i_y n_y^2+2N^i_{xy}n_x n_y,\\
&N^i_s=\left(N^i_y-N^i_x\right)n_x n_y+N^i_{xy}\left(n_x^2-n_y^2\right),\\
&Q^i_n=Q^i_x n_x+Q^i_y n_y,\quad i=\overline{1,I};
\end{aligned}
$$

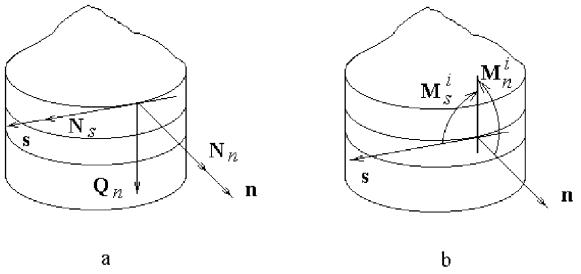

a b

Fig. 2. Forces and moments on boundary L.

M_n^i and M_s^i are bending and torque moments in the ith layer, respectively (Fig. 2b),

$$M_n^i = M_x^i n_x^2 + M_y^i n_y^2 + 2M_{xy}^i n_x n_y + h_i \sum_{j=i}^{I-1} \left(N_x^{j+1} n_x^2 + N_y^{j+1} n_y^2 + 2N_{xy}^{j+1} n_x n_y \right),$$

$$M_s^i = \left(M_y^i - M_x^i \right) n_x n_y + M_{xy}^i \left(n_x^2 - n_y^2 \right) + h_i \sum_{j=i}^{I-1} \left[\left(N_y^{j+1} - N_x^{j+1} \right) n_x n_y + N_{xy}^{j+1} \left(n_x^2 - n_y^2 \right) \right], \quad i = \overline{1, I},$$

$n_x = \cos(x, \mathbf{n})$, $n_y = \cos(y, \mathbf{n})$ are directional cosines of the normal $\mathbf{n}$ to boundary L.

The coefficients $\varsigma_{kl} (k = \overline{1, 2I+3}, l = 1, 2)$ allow simulating particular boundary conditions on boundary L. For example, in the case of a simply supported plate

$$\begin{aligned} &\varsigma_{11} = \varsigma_{22} = \varsigma_{32} = \varsigma_{3+i,1} = \varsigma_{3+I+i,2} = 1, \\ &\varsigma_{12} = \varsigma_{21} = \varsigma_{31} = \varsigma_{3+i,2} = \varsigma_{3+I+i,1} = 0, \quad i = \overline{1, I}. \end{aligned} \tag{9}$$

Eqs. (3)–(6) enable us to write the system (7) and boundary conditions (8) in terms of functions of the displacements.

So, the dynamic boundary problem is described by the equations of motion

$$\mathbf{M}\mathbf{U}_{,tt} + \mathbf{S}\mathbf{U} = \mathbf{P}^{\mathrm{e}}, \quad x, y \in \Omega, \tag{10}$$

conditions on the curvilinear boundary L

$$\mathbf{B}^L \mathbf{U} = 0, \quad x, y \in L, \tag{11}$$

and initial conditions

$$\mathbf{U} = \mathbf{U}_{,t} = 0, \quad t = 0, \tag{12}$$

where $\mathbf{M}$, $\mathbf{S}$ and $\mathbf{B}^L$ are square matrices of dimension $(2I+3) \times (2I+3)$;

$$\begin{aligned} &\mathbf{U} = \{u_i\}, \quad u_1 = u(x, y, t), \quad u_2 = v(x, y, t), \quad u_3 = w(x, y, t), \\ &u_{3+i} = \psi_x^i(x, y, t), \quad u_{3+I+i} = \psi_y^i(x, y, t), \quad i = \overline{1, I}. \end{aligned}$$

The elements of matrix $\mathbf{M}$ are equal to zero, except $m_{33} = -C_\rho^I (\partial^2 / \partial t^2)$, $C_\rho^I = \sum_{i=1}^I \rho_i h_i$. The elements of matrix $\mathbf{S}$ are presented in Appendix A. The elements of matrix $\mathbf{B}^L$ determining the boundary conditions have the form

$$b_{kl}^L = \varsigma_{k1} b_{kl}^1 + \varsigma_{k2} b_{kl}^2, \quad k, l = \overline{1, 2I+3}. \tag{13}$$

The elements b_{kl}^1 and b_{kl}^2 are given in Appendix B.

The boundary conditions for a rectangular simply supported plate are derived from relationship (13) in view of Eq. (9) at the following directional cosines (see Appendix B):

$$\begin{aligned} &x = 0, \quad x = A, \quad n_x = 1, \quad n_y = 0, \\ &y = 0, \quad y = B, \quad n_x = 0, \quad n_y = 1, \end{aligned} \tag{14}$$

where A and B are geometric dimensions of a plate.

3. Elastic immersion method

3.1. Problem statement

The original plate is immersed into an auxiliary enveloping plate having an identical layer composition. An auxiliary plate occupies domain Ω_E, $\Omega \subset \Omega_E$ in the plane $x0y$ (Fig. 3). The enveloping plate is loaded within the limits of domain Ω the same way as the given plate.

The contour L_E of enveloping plate and boundary conditions are selected so that it is possible to obtain a simple analytical solution. In the present paper the auxiliary plate is a rectangular simply supported plate. In this case the problem solution can be obtained in the form of trigonometrical series.

To ensure fulfillment of actual boundary conditions to an auxiliary plate on a trace of boundary L some additional compensatory forces and moments $\mathbf{Q}^{\mathrm{c}} = \{q_j^{\mathrm{c}}(x,y,t)\}$, $j = \overline{1, 2I+3}$, $x, y \in L$ are applied.

Hence, the initial problem (10)–(12) of vibration of the plate Ω affected by an impulse load $\mathbf{P}^{\mathrm{e}}$ is reduced to the problem of vibration of the rectangular plate Ω_E under the action of a known load $\mathbf{P}^{\mathrm{e}}$ and compensatory loads $\mathbf{Q}^{\mathrm{c}}$ specified as curvilinear distributions $\mathbf{P}^{\mathrm{c}} = \{p_j^{\mathrm{c}}(x,y,t)\}$, $j = \overline{1, 2I+3}$

$$\mathbf{P}^{\mathrm{c}}(x,y,t) = \int_{\varphi_0}^{\varphi_1} \mathbf{Q}^{\mathrm{c}}(\varphi,t)\,\delta(x-x_L, y-y_L)\Gamma(\varphi)\,\mathrm{d}\varphi, \tag{15}$$

where $\delta(x-x_L,\ y-y_L)$ is the two-dimensional Dirac delta-function,

$$\Gamma(\varphi) = \left[(\dot{x}_L)^2 + (\dot{y}_L)^2\right]^{1/2},\ \ \dot{x}_L = \frac{\mathrm{d}x_L}{\mathrm{d}\varphi},\ \ \dot{y}_L = \frac{\mathrm{d}y_L}{\mathrm{d}\varphi}.$$

The vibration of the auxiliary plate Ω_E is described by the equations of motion

$$\mathbf{M}\mathbf{U}_{,tt} + \mathbf{S}\mathbf{U} = \mathbf{P}^{\mathrm{e}} + \mathbf{P}^{\mathrm{c}},\ \ x, y \in \Omega_E, \tag{16}$$

boundary conditions

$$\mathbf{B}^E\mathbf{U} = 0,\ \ x, y \in L_E, \tag{17}$$

conditions on a trace of the boundary L

$$\mathbf{B}^L\mathbf{U} = 0,\ \ x, y \in L, \tag{18}$$

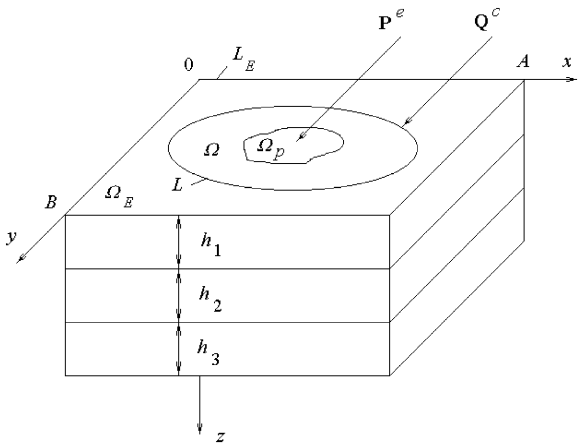

Fig. 3. Auxiliary enveloping plate.

and initial conditions

$$\mathbf{U} = \mathbf{U}_{,t} = 0, \quad t = 0, \tag{19}$$

where the elements of matrix $\mathbf{B}^E$ are derived from Eq. (11) with allowance for Eqs. (9), (13) and (14). The sought-for functions of the boundary problem formulated are the components of vectors of displacements $\mathbf{U}$ and compensatory loads $\mathbf{Q}^{\mathrm{c}}$.

The system of equations (16) and the conditions (17)–(19) allow to establish a relation

$$\mathbf{U} = \mathbf{U}[\mathbf{Q}^{\mathrm{c}}(x, y, t)] \tag{20}$$

and to generate a system of $2I + 3$ integral equations for definition of compensatory forces and moments

$$\mathbf{B}^L \mathbf{U}[\mathbf{Q}^{\mathrm{c}}(x, y, t)] = 0, \quad x, y \in L. \tag{21}$$

The compensatory forces and moments $\mathbf{Q}^{\mathrm{c}}$ enter in the system (21) as integral relations (15).

The equations of motion of the given Eq. (10) and auxiliary (16) plates inside the domain Ω are identical. The conditions on a trace of the boundary L (18) and boundary conditions of the given plate (11) identically coincide. Identical loads $\mathbf{P}^{\mathrm{e}}$ affect the enveloping and the given plates in the domain Ω. Consequently, a boundary problem solution (16)–(19) for the auxiliary plate Ω_E inside the domain $\Omega \subset \Omega_E$ identically coincides with a boundary problem solution (10)–(12) for the initial plate.

3.2. Method of solution

Loads $\mathbf{P}^{\mathrm{e}}$ and $\mathbf{P}^{\mathrm{c}}$ as well as displacements $\mathbf{U}$ are expanded into trigonometrical series in domain Ω_E by functions satisfying simply supported conditions (17) on the boundary L_E

$$\begin{aligned}
u_j(x, y, t) &= \sum_{m=l}^{\infty} \sum_{n=l}^{\infty} \phi_{jmn}(t)\, B_{jmn}(x, y), \\
p^{\mathrm{e}}(x, y, t) &= \sum_{m=l}^{\infty} \sum_{n=l}^{\infty} p^{\mathrm{e}}_{jmn}(t)\, B_{jmn}(x, y), \\
p^{\mathrm{c}}_j(x, y, t) &= \sum_{m=l}^{\infty} \sum_{n=l}^{\infty} p^{\mathrm{c}}_{jmn}(t)\, B_{jmn}(x, y), \quad j = \overline{1, 2I + 3},
\end{aligned} \tag{22}$$

where

$$\begin{aligned}
&B_{1mn} = \cos\frac{m\pi x}{A} \sin\frac{n\pi y}{B}, \qquad B_{2mn} = \sin\frac{m\pi x}{A} \cos\frac{n\pi y}{B}, \\
&B_{3mn} = \sin\frac{m\pi x}{A} \sin\frac{n\pi y}{B}, \qquad B_{3+i,mn} = B_{1mn}, \\
&B_{3+I+i,mn} = B_{2mn}, \quad i = \overline{1, I}.
\end{aligned}$$

The coefficients of expansion of an external load have the following form:

$$\begin{aligned}
&p^{\mathrm{e}}_{1mn} = p^{\mathrm{e}}_{2mn} = p^{\mathrm{e}}_{3+i,mn} = p^{\mathrm{e}}_{3+I+i,mn} = 0, \quad i = \overline{1, I}, \\
&p^{\mathrm{e}}_{3mn}(t) = \frac{4}{AB} \int\int_{\Omega_p} p^{\mathrm{e}}_3(x, y, t) B_{3mn}(x, y)\, \mathrm{d}x\, \mathrm{d}y.
\end{aligned} \tag{23}$$

The coefficients of expansion for $\mathbf{P}^{\mathrm{c}}$ [see Eq. (15)] can be written as

$$p^{\mathrm{c}}_{jmn}(t) = \frac{4}{AB} \int_{\varphi_0}^{\varphi_1} q^{\mathrm{c}}_j(\varphi, t) B_{jmn}(x_L, y_L) \Gamma(\varphi)\, \mathrm{d}\varphi. \tag{24}$$

In doing so, the following properties of the Dirac delta-function are taken into account:

$$\delta(x-x_0,y-y_0)=\delta(x-x_0)\,\delta(y-y_0),$$
$$\int_\alpha^\beta f(x)\,\delta(x-x_0)\,\mathrm{d}x=f(x_0).$$

Thus, the system of equations (16) for each pair of values m and n becomes

$$\mathbf{M}^{mn}\ddot{\mathbf{\Phi}}_{mn}+\mathbf{\Lambda}^{mn}\mathbf{\Phi}_{mn}=\mathbf{P}^{\mathrm{e}}_{mn}+\mathbf{P}^{\mathrm{c}}_{mn}, \tag{25}$$

where $\mathbf{M}^{mn}$ and $\mathbf{\Lambda}^{mn}$ are square matrices,

$$\mathbf{P}^{\mathrm{e}}_{mn}=\{p^{\mathrm{e}}_{jmn}\},\quad \mathbf{P}^{\mathrm{c}}_{mn}=\{p^{\mathrm{c}}_{jmn}\},\quad \mathbf{\Phi}_{mn}=\{\phi_{jmn}\},\ \ j=\overline{1,2I+3}.$$

The elements of matrix $\mathbf{M}^{mn}$ are equal to zero except for $m^{mn}_{33}=C^I_\rho$. The elements of matrix $\mathbf{\Lambda}^{mn}$ are given in Appendix C.

Since in the system (25) only the inertia of motion in transverse direction is taken into account, it can be presented as a single differential equation

$$C^I_\rho\ddot{\phi}_{3mn}+\sum_{j=1}^{2I+3}\lambda^{mn}_{3j}\phi_{jmn}=p^{\mathrm{e}}_{3mn}+p^{\mathrm{c}}_{3mn} \tag{26}$$

with initial conditions

$$\phi_{3mn}(0)=\dot{\phi}_{3mn}(0)=0,$$

and $2I+2$ algebraic equations

$$\hat{\mathbf{\Lambda}}^{mn}\hat{\mathbf{\Phi}}_{mn}=\hat{\mathbf{P}}^{\mathrm{c}}_{mn}+\hat{\mathbf{V}}_{mn}\phi_{3mn}. \tag{27}$$

The matrix $\hat{\mathbf{\Lambda}}^{mn}$ is obtained from $\mathbf{\Lambda}^{mn}$ by striking out the third column and third row. The vectors $\hat{\mathbf{\Phi}}_{mn}$ and $\hat{\mathbf{P}}^{\mathrm{c}}_{mn}$ turn out from vectors $\mathbf{\Phi}_{mn}$ and $\mathbf{P}^{\mathrm{c}}_{mn}$, respectively, by deletion of the third element. The vector $\hat{\mathbf{V}}_{mn}$ is obtained from the third column of a matrix $\mathbf{\Lambda}^{mn}$ by deletion of element λ^{mn}_{33}.

The system (27) enables us to express coefficients $\phi_{jmn}(t),(j=\overline{1,2I+3},j\neq 3)$ through $\phi_{3mn}(t)$

$$\hat{\mathbf{\Phi}}_{mn}=\tilde{\mathbf{\Lambda}}^{mn}\hat{\mathbf{P}}^{\mathrm{c}}_{mn}+\tilde{\mathbf{V}}_{mn}\phi_{3mn},$$

where

$$\tilde{\mathbf{\Lambda}}^{mn}=\hat{\mathbf{\Lambda}}^{mn^{-1}},\qquad \tilde{\mathbf{V}}_{mn}=\tilde{\mathbf{\Lambda}}^{mn}\hat{\mathbf{V}}_{mn}.$$

As a result, the coefficients of expansion of the displacements reduce to

$$\mathbf{\Phi}_{mn}=\mathbf{\Gamma}^{mn}\mathbf{P}^{\mathrm{c}}_{mn}+\mathbf{V}_{mn}\phi_{3mn}, \tag{28}$$

where

$$\gamma^{mn}_{ik}=\tilde{\lambda}^{mn}_{ik},\quad \gamma^{mn}_{i,3+j}=\tilde{\lambda}^{mn}_{i,2+j},\ \ i,k=1,2,\ \ j=\overline{1,2I},$$
$$\gamma^{mn}_{3i}=\gamma^{mn}_{i3}=0,\ \ i=\overline{1,2I+3},$$
$$\gamma^{mn}_{3+i,3+j}=\tilde{\lambda}^{mn}_{2+i,2+j},\ \ i,j=\overline{1,2I},$$
$$v_{imn}=\tilde{v}_{imn},\quad v_{3mn}=1,\quad v_{3+j,mn}=\tilde{v}_{2+j,mn},\ \ i=1,2,\ \ j=\overline{1,2I}.$$

The relationship (28) allows transforming Eq. (26) to the form

$$\ddot{\phi}_{3mn} + \omega_{mn}^2 \phi_{3mn} = \frac{1}{C_\rho^I}\left(p_{3mn}^{\mathrm{e}} + \sum_{j=1}^{2I+3} \delta_{jmn} p_{jmn}^{\mathrm{c}}\right), \tag{29}$$

where

$$\omega_{mn}^2 = \frac{1}{C_\rho^I}\sum_{j=1}^{2I+3} \lambda_{3j}^{mn} v_{jmn},$$

$$\delta_{3mn} = 1, \quad \delta_{imn} = -\sum_{j=1}^{2I+3} \lambda_{3j}^{mn}\gamma_{ji}^{mn}, \quad i = \overline{1, 2I+3}, \quad i \neq 3.$$

The solution of Eq. (29) in view of the initial conditions (26) is obtained by using the Laplace integral transform

$$\phi_{3mn}(t) = \phi_{3mn}(t_0)\cos\left[\omega_{mn}(t-t_0)\right] + \dot{\phi}_{3mn}(t_0)\frac{\sin\left[\omega_{mn}(t-t_0)\right]}{\omega_{mn}} + \frac{1}{C_\rho^I \omega_{mn}}\int_{t_0}^{t}\left[p_{3mn}^{\mathrm{e}}(\tau) + \sum_{i=1}^{2I+3}\delta_{imn} p_{imn}^{\mathrm{c}}(\tau)\right]\sin\left[\omega_{mn}(t-\tau)\right]\mathrm{d}\tau.$$

Putting $t_0 = s\Delta t$, where $\Delta t = t - t_0$ is a step on time (Smetankina et al., 1995), this solution can be represented in the form of recurrence formulas

$$\phi_{3mn}^{s+1} = \eta_{11}\phi_{3mn}^{s} + \eta_{12}\dot{\phi}_{3mn}^{s} + \eta_{13} p_{3mn}^{\mathrm{e},s+1} + \sum_{i=1}^{2I+3}\eta_{1i}^{\mathrm{c}} p_{imn}^{\mathrm{c},s+1},$$

$$\dot{\phi}_{3mn}^{s+1} = \eta_{21}\phi_{3mn}^{s} + \eta_{22}\dot{\phi}_{3mn}^{s} + \eta_{23} p_{3mn}^{\mathrm{e},s+1} + \sum_{i=1}^{2I+3}\eta_{2i}^{\mathrm{c}} p_{imn}^{\mathrm{c},s+1}.$$

Here

$$\eta_{11} = C, \quad \eta_{12} = \frac{S}{\omega_{mn}}, \quad \eta_{13} = \frac{1-C}{C_\rho^I \omega_{mn}^2}, \quad \eta_{1i}^{\mathrm{c}} = \eta_{13}\delta_{imn},$$

$$\eta_{21} = -S\omega_{mn}, \quad \eta_{22} = C, \quad \eta_{23} = \frac{S}{C_\rho^I \omega_{mn}}, \quad \eta_{2i}^{\mathrm{c}} = \eta_{23}\delta_{imn},$$

$$C = \cos(\omega_{mn}\Delta t), \qquad S = \sin(\omega_{mn}\Delta t).$$

The recurrence formulas enable us to write coefficients of expansion of the displacements (22) in the final form

$$\phi_{imn}^{s+1} = \sum_{j=1}^{2I+3}\pi_{ij}^{mn} p_{jmn}^{\mathrm{c},s+1} + \varepsilon_{imn}^{s+1}, \quad i = \overline{1, 2I+3}, \tag{30}$$

where

$$\pi_{ij}^{mn} = \gamma_{ij}^{mn} + v_{imn}\eta_{ij}^{\mathrm{c}},$$

$$\varepsilon_{imn}^{s+1} = v_{imn}\left(\eta_{11}\phi_{3mn}^{s} + \eta_{12}\dot{\phi}_{3mn}^{s} + \eta_{13} p_{3mn}^{\mathrm{e},s+1}\right).$$

Thus, the relation between displacements and compensatory loads on each step on time is established.

3.3. Determination of compensatory loads

Compensatory loads are determined from the system of integral equations (21). As in the paper by Zielinski (1985), compensatory forces and moments $\mathbf{Q}^{c}$ are expanded into a single series along a trace of the boundary L

$$q_j^{c}(\varphi,t)=\sum_{\alpha=1,2}\sum_{\mu=0}^{\infty}f_{j\alpha\mu}(t)d_{\alpha\mu}(\varphi),\quad j=\overline{1,2I+3}, \tag{31}$$

where

$$d_{1\mu}=\sin[\mu\gamma(\varphi)],\qquad d_{2\mu}=\cos[\mu\gamma(\varphi)],$$
$$\gamma(\varphi)=2\pi(\varphi-\varphi_0)/(\varphi_1-\varphi_0),\quad 0\leqslant\gamma(\varphi)\leqslant 2\pi.$$

With allowance for Eq. (31) the coefficients (24) are transformed to the form

$$p_{jmn}^{c}=\sum_{\alpha=1,2}\sum_{\mu=0}^{\infty}f_{j\alpha\mu}(t)\theta_{j\alpha\mu}^{mn},\quad j=\overline{1,2I+3}, \tag{32}$$

where

$$\theta_{j\alpha\mu}^{mn}=\frac{4}{AB}\int_{\varphi_0}^{\varphi_1}d_{\alpha\mu}(\varphi)B_{jmn}(x_L,y_L)\Gamma(\varphi)\,\mathrm{d}\varphi,$$

and the coefficients (30) are written as

$$\phi_{imn}^{s+1}=\sum_{j=1}^{2I+3}\sum_{\alpha=1,2}\sum_{\mu=0}^{\infty}\pi_{ij}^{mn}\theta_{j\alpha\mu}^{mn}f_{j\alpha\mu}^{s+1}+\varepsilon_{imn}^{s+1},\quad i=\overline{1,2I+3}. \tag{33}$$

The displacement functions $\mathbf{U}$ entering in Eq. (21) also are expanded into series along a trace of the boundary L. As a result, the system (21) takes the form

$$\sum_{\alpha=1,2}\sum_{\mu=0}^{\infty}\xi_{i\alpha\mu}(t)\,d_{\alpha\mu}(\varphi)=0. \tag{34}$$

Here

$$\xi_{i\alpha\mu}(t)=\frac{1}{\lambda_\mu}\sum_{k=1}^{2I+3}\int_{\varphi_0}^{\varphi_1}b_{ik}^{L}u_k(\varphi)\,d_{\alpha\mu}(\varphi)\,\mathrm{d}\varphi,\quad i=\overline{1,2I+3},\quad \alpha=1,2,$$
$$\lambda_\mu=\varphi_1-\varphi_0,\quad \mu=0;\quad \lambda_\mu=(\varphi_1-\varphi_0)/2,\quad \mu=1,2,\ldots$$

The conditions (34) are satisfied for all values $\varphi,\varphi\in[\varphi_0,\varphi_1]$ when

$$\xi_{i\alpha\mu}(t)=0,\quad i=\overline{1,2I+3},\quad \alpha=1,2,\quad \mu=0,1,\ldots \tag{35}$$

The relationships (32), (33) and (35) allow reducing the system of integral equations (21) to a system of algebraic equations

$$\sum_{j=1}^{2I+3}\sum_{\beta=1,2}\sum_{\nu=0}^{\infty}\tau_{i\alpha\mu j\beta\nu}f_{j\beta\nu}^{s+1}=r_{i\alpha\mu}^{s+1},\quad i=\overline{1,2I+3},\quad \alpha=1,2,\quad \mu=0,1,\ldots, \tag{36}$$

where

$$\tau_{i\alpha\mu j\beta\nu} = \varsigma_{i1}\left[\sum_{m=1}^{\infty}\sum_{n=1}^{\infty}\theta_{j\beta\nu}^{mn}\sum_{k=1}^{2I+3}\pi_{kj}^{mn}\chi_{ik\alpha\mu}^{1mn} + \frac{\delta_{ij}}{2}\right] + \varsigma_{i2}\left[\sum_{m=1}^{\infty}\sum_{n=1}^{\infty}\theta_{j\beta\nu}^{mn}\sum_{k=1}^{2I+3}\pi_{kj}^{mn}\chi_{ik\alpha\mu}^{2mn}\right],$$

$$r_{i\alpha\mu}^{s+1} = \varsigma_{i1}\left[-\sum_{m=1}^{\infty}\sum_{n=1}^{\infty}\sum_{k=1}^{2I+3}\varepsilon_{kmn}^{s+1}\chi_{ik\alpha\mu}^{1mn}\right] + \varsigma_{i2}\left[-\sum_{m=1}^{\infty}\sum_{n=1}^{\infty}\sum_{k=1}^{2I+3}\varepsilon_{kmn}^{s+1}\chi_{ik\alpha\mu}^{2mn}\right],$$

$$\delta_{ij} = \begin{cases} 1, & i = 1 \\ 0, & i \neq j \end{cases} \text{ being the Kronecker delta,}$$

$$\chi_{ik\alpha\mu}^{1mn} = \frac{1}{\lambda_\mu}\int_{\varphi_0}^{\varphi_1} b_{ik}^1 B_{kmn}(x_L, y_L) d_{\alpha\mu}(\varphi)\,\mathrm{d}\varphi,$$

$$\chi_{ik\alpha\mu}^{2mn} = \frac{1}{\lambda_\mu}\int_{\varphi_0}^{\varphi_1} b_{ik}^2 B_{kmn}(x_L, y_L) d_{\alpha\mu}(\varphi)\,\mathrm{d}\varphi, \quad i,k = \overline{1, 2I+3}, \quad \alpha = 1,2, \quad \mu = 0,1,\ldots$$

Eqs. (36) are solved on each step on time. The order of the system (36) depends on the number of layers in a plate and the number of terms of series taken into account in expansions (31) and (34). After calculation of coefficients $f_{j\beta\nu}^{s+1}$ we find the values of compensatory loads (31). Finally, the displacements and stresses in layers of the given plate Ω are determined by formulas (33), (22), (3) and (5).

4. Numerical results

The functionality of the method proposed is illustrated by examples of investigating the strain-stressed state of simply supported plates with boundary given by equations of Lamé's curves (Fig. 4)

$$\begin{aligned} x(\varphi) &= A/2 + \alpha\cos^{2/q}(\varphi), \\ y(\varphi) &= B/2 + \beta\sin^{2/q}(\varphi). \end{aligned} \tag{37}$$

If $q = 2$ and $\alpha \neq \beta$, Eqs. (37) describe an ellipse with point $x = A/2$, $y = B/2$ as its centre and semi-axes α and β (line 1 in Fig. 4). At increasing parameter q Lamé's curves approach asymptotically to a rectangle with sides 2α and 2β. Lines 2 and 3 correspond to $q = 4$ and $q = 10$, respectively.

An impulse load (2) is uniformly distributed over a circular area with radius R and changes in time according to the law

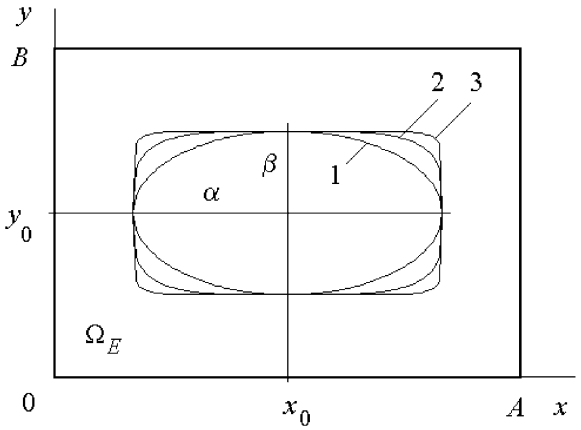

Fig. 4. Lamé's curves.

$$p_3^{\mathrm{e}} = \frac{1}{2}P_0[1 + \operatorname{sgn}(t_1 - t)] \sin^2\left(\frac{\pi t}{t_1}\right), \tag{38}$$

where P_0 is load intensity, t_1 is impulse duration. The coefficients of expansion of the load (38) into Fourier series (23) have the form

$$p_{3mn}^{\mathrm{e}} = \frac{8P_0 J_1(R\gamma_{mn})}{ABR\gamma_{mn}} \sin\left(\frac{m\pi x_0}{A}\right) \sin\left(\frac{n\pi y_0}{B}\right)[1 + \operatorname{sgn}(t_1 - t)] \sin^2\left(\frac{\pi t}{t_1}\right),$$

where x_0, y_0 are coordinates of centre of loaded area,

$$\gamma_{mn} = \left[\left(\frac{m\pi}{A}\right)^2 + \left(\frac{n\pi}{B}\right)^2\right]^{1/2}.$$

A three-layer plate is considered. The plate has the following parameters: $q = 10$, $\alpha = \beta = 0.25$ m, $h_1 = h_3 = 10^{-2}$ m, $h_2 = 5 \times 10^{-3}$ m, $E_1 = E_3 = 6.12 \times 10^4$ MPa, $E_2 = 2.8 \times 10^2$ MPa, $\nu_1 = \nu_3 = 0.22, \nu_2 = 0.38$, $\rho_1 = \rho_3 = 2.5 \times 10^3$ kg m^{-3}, $\rho_2 = 1.2 \times 10^3$ kg m^{-3}.

The load characteristics (38) are $R = 2 \times 10^{-2}$ m, $P_0 = 2$ MPa, $t_1 = 5 \times 10^{-3}$ s, $x_0 = A/2$, $y_0 = B/2$. Stresses are calculated at the point with coordinates $x_c = A/2$, $y_c = B/2$, $z_c = \delta_3$.

Table 1
Influence of dimensions of the enveloping domain upon convergence of the solution

$A/(2\alpha)$	$m_w^* = n_w^*$	μ_w^*	$m_\sigma^* = n_\sigma^*$	μ_σ^*
2	30	4	35	4
4	60	8	70	8
6	100	8	110	8
8	130	12	140	12
10	140	12	160	12

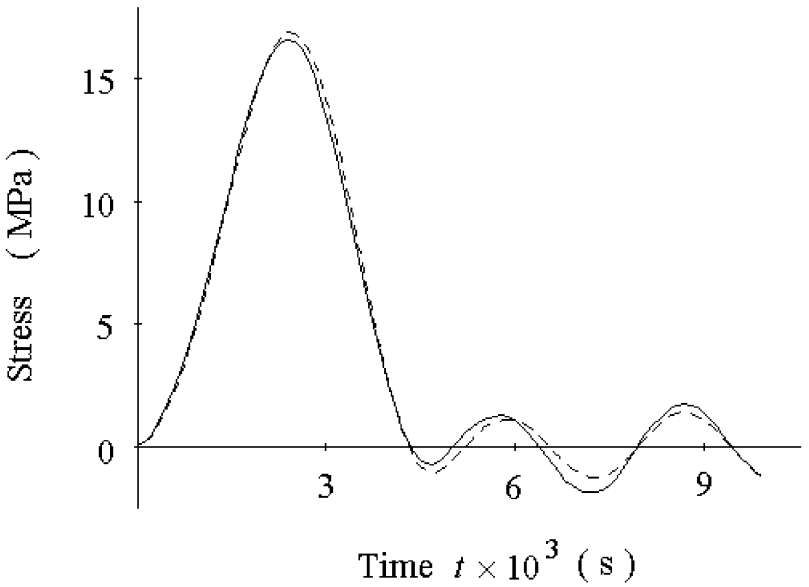

Fig. 5. Stress σ_x^3 in a three-layer plate, $q = 10$.

The influence of dimensions of the enveloping plate upon convergence of the solution was studied. The number of terms in expansions (22) $\left(m_w^*, n_w^*, m_\sigma^*, n_\sigma^*\right)$ and in expansions (31) $\left(\mu_w^*, \mu_\sigma^*\right)$ are given in Table 1. At their further increase the change of the maximum deflections does not exceed 0.5% and that of stresses 1%. That is at $m > m_w^*, n > n_w^*, \mu > \mu_w^*$

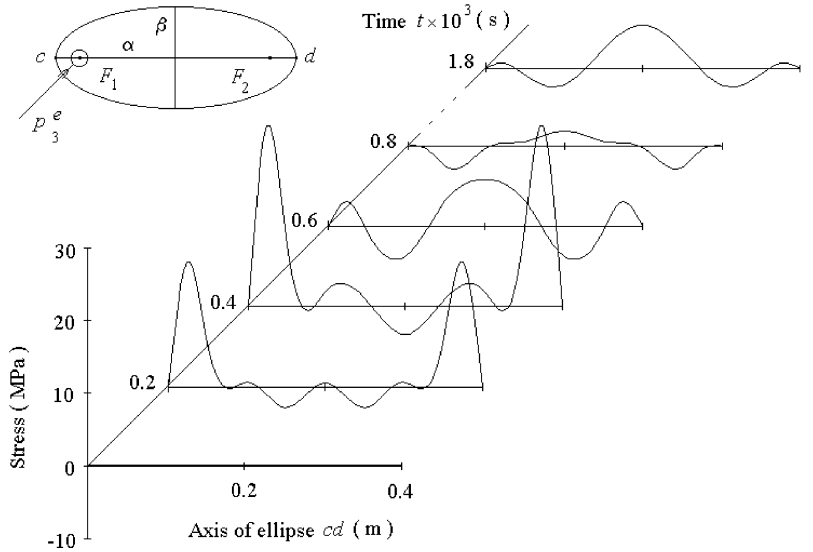

Fig. 6. Distribution of stresses σ_x^3 along the axis of elliptical plate.

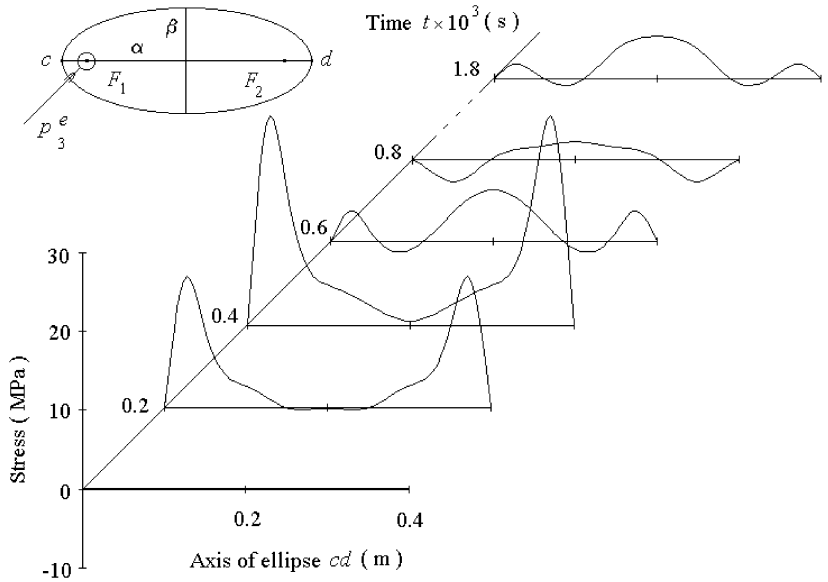

Fig. 7. Distribution of stresses σ_y^3 along the axis of elliptical plate.

$$\left| \frac{w^{\max}|_{m,n,\mu} - w^{\max}|_{m_w^*,n_w^*,\mu_w^*}}{w^{\max}|_{m_w^*,n_w^*,\mu_w^*}} \right| \times 100\% \leqslant 0.5\%,$$

and at $m > m_\sigma^*$, $n > n_\sigma^*$, $\mu > \mu_\sigma^*$

$$\left| \frac{\sigma^{\max}|_{m,n,\mu} - \sigma^{\max}|_{m_\sigma^*,n_\sigma^*,\mu_\sigma^*}}{\sigma^{\max}|_{m_\sigma^*,n_\sigma^*,\mu_\sigma^*}} \right| \times 100\% \leqslant 1\%.$$

Henceforth it is taken $A = B = 1$ m.

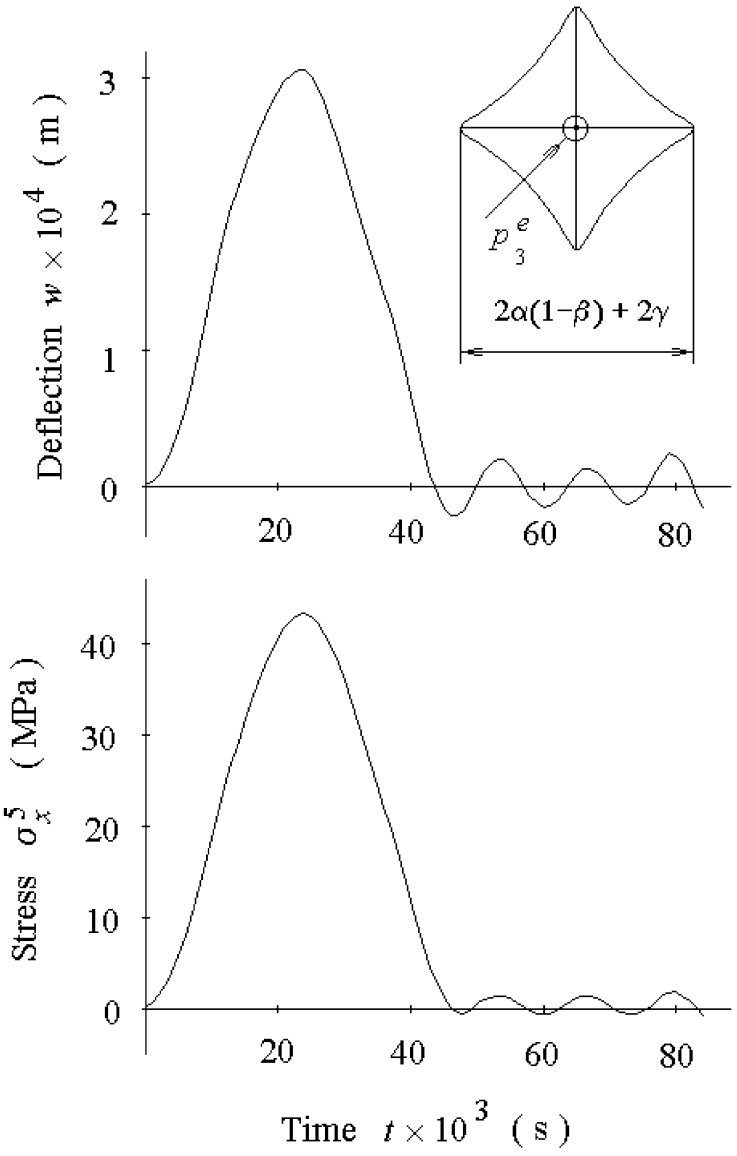

Fig. 8. Deflection and stresses in a five-layer plate.

Fig. 5 shows the variation of stresses in time for the plate described above (the solid line). The dashed line shows similar dependence for a square plate obtained by a technique proposed by Smetankina et al. (1995). It may be noted that the dependences presented are closely spaced. It confirms the reliability of the results obtained by the method offered.

A three-layer elliptical plate with parameters $q = 2$, $\alpha = 0.2$ m, $\beta = 0.1$ m, $h_i = 5 \times 10^{-3}$ m $(i = 1, 2, 3)$ is considered. The mechanical properties of layer materials are the same as in the previous case. The characteristics of impulse load (38) have the following values: $R = 10^{-2}$ m, $P_0 = 10$ MPa, $t_1 = 7 \times 10^{-4}$ s. The central point of loaded area coincides with the focus of the ellipse $x_0 = A/2 - (\alpha^2 - \beta^2)^{1/2}$; $y_0 = B/2$.

The distribution of normal stresses along an axis of the elliptical plate at different instants of time was studied: $\sigma_x^3 = \sigma_x^3(x, y, z, t)$, $\sigma_y^3 = \sigma_y^3(x, y, z, t)$, $A/2 - \alpha \leqslant x \leqslant A/2 + \alpha$, $y = B/2$, $z = \delta_3$, $t = t_k$. The calculation results are presented in Figs. 6 and 7. The effect of concentration of maximum stresses in both focal points of the plate in the instant of time $t = 4 \times 10^{-4}$ s has been detected. Stress concentration in both focal points of an elliptical plate when the load is applied only in one focal point is explained by effect of reflection of flexural waves from the elliptical boundary of a plate and their subsequent concentration in focal points.

The next example studies the case of a five-layer plate with the boundary given by equations of hypotrochoid

$$x(\varphi) = A/2 + \alpha(1 - \beta)\cos(\beta\varphi) + \gamma\cos[(1 - \beta)\varphi],$$
$$y(\varphi) = B/2 + \alpha(1 - \beta)\sin(\beta\varphi) - \gamma\sin[(1 - \beta)\varphi],$$

where $\alpha = 0.4$ m, $\beta = 0.25$, $\gamma = 7 \times 10^{-2}$ m.

The plate is subjected to the impulsive load (38). The characteristics of load and plate are $R = 2 \times 10^{-2}$ m, $P_0 = 10$ MPa, $t_1 = 5 \times 10^{-3}$ s, $x_0 = A/2$, $y_0 = B/2$, $h_1 = h_3 = h_5 = 10^{-2}$ m, $h_2 = h_4 = 5 \times 10^{-3}$ m, $E_1 = E_3 = E_5 = 6.12 \times 10^4$ MPa, $E_2 = E_4 = 2.8 \times 10^2$ MPa, $\nu_1 = \nu_3 = \nu_5 = 0.22$, $\nu_2 = \nu_4 = 0.38$, $\rho_1 = \rho_3 = \rho_5 = 2.5 \times 10^3$ kg m^{-3}, $\rho_2 = \rho_4 = 1.2 \times 10^3$ kg m^{-3}. Stresses are calculated at the point with coordinates $x_c = A/2$, $y_c = B/2$, $z_c = \delta_5$. Fig. 8 shows the time dependences of deflection and stresses in the plate.

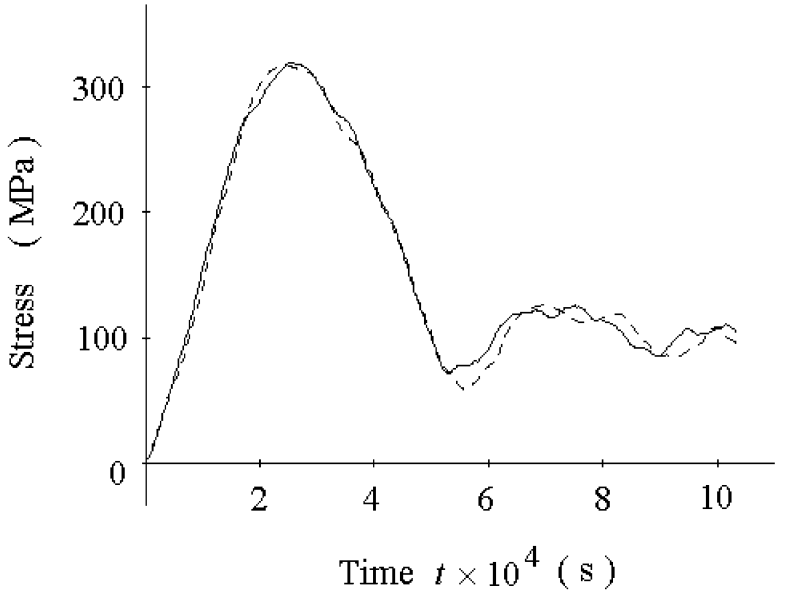

Fig. 9. Variation of stress σ_r in a round plate under impact.

A single-layer steel round plate subjected to an impact load is considered. Parameters of the plate are $q = 2$, $\alpha = \beta = 0.287$ m, $h = 3 \times 10^{-2}$ m. Loading is effected by dropping a steel ball with the mass of 18.2 kg from the height of 0.26 m in the centre of the plate ($x_0 = A/2$, $y_0 = B/2$, $z_0 = 0$). The mechanical properties of the plate and the ball are as follows: $E = 2.1 \times 10^5$ MPa, $v = 0.3$, $\rho = 7.85 \times 10^3$ kg m^{-3}.

The impact is described in the same manner as in the work of Smetankina et al. (1995). The contact approach of bodies is determined by Hertz's theory. Stresses are calculated in the centre of the plate at $z = h$.

In Fig. 9 the variation of stress σ_r (the solid line) is shown. The dashed line shows similar dependence obtained in the work of Goloskokov and Filippov (1977) by using symbolical method and expanding the solution into a series by Bessel functions. It should be noted that the dependences obtained in both cases practically coincide.

5. Conclusions

A method of investigating non-stationary vibration of multilayer plates of an arbitrary plan form under impulse and impact loading has been developed.

The method is based on application of boundary integral equations. However, as distinct from the known similar approaches, at solving a system of integral equations instead of discretization of the boundary of a plate, the unknown boundary functions are expanded into trigonometrical series along contour of this plate. It considerably simplifies the preparation of input data in computations and improves the accuracy of a problem solution.

The dynamic behaviour of multilayer plates is described by the first-order refined theory. For a pack of layers the broken line hypothesis is accepted.

The possibilities of the method are demonstrated by examples of analysis of the strain-stressed state of multilayer plates, their contour being described by Lamé's curves. Such selection of the contour, without a loss a generality, allows to confirm reliability of results by a comparison with the similar data obtained by other methods. A five-layer plate with contour given by equations of hypotrochoid is presented in order to demonstrate the range of application of the elastic immersion method to the plate-bending problem.

The internal convergence of the method presented has been studied. In case where the form of Lamé's curve comes nearer to rectangular, a comparison with the data obtained for a square plate by other technique has been performed. The calculation results for a single-layer round plate under impact loading are compared with the similar data by other authors. In all cases the comparative analysis of dependences shows their coincidence that confirms reliability of results obtained by the method proposed.

For an elliptical plate under an impulse localized load applied at the focus the effect of concentration of maximum stresses in both focuses is shown.

Appendix A

$$s_{11} = C_1^l \frac{\partial^2}{\partial x^2} + C_3^l \frac{\partial^2}{\partial y^2}, \quad s_{12} = s_{21} = \left(C_2^l + C_3^l\right) \frac{\partial^2}{\partial x \partial y},$$

$$s_{13} = s_{31} = 0, \quad s_{1,3+i} = s_{3+i,1} = D_1^i \frac{\partial^2}{\partial x^2} + D_3^i \frac{\partial^2}{\partial y^2},$$

$$s_{1,3+I+i} = s_{3+I+i,1} = \left(D_2^i + D_3^i\right) \frac{\partial^2}{\partial x \partial y},$$

$$s_{22} = C_3^I \frac{\partial^2}{\partial x^2} + C_1^I \frac{\partial^2}{\partial y^2}, \quad s_{23} = s_{32} = 0,$$

$$s_{2,3+i} = s_{3+i,2} = \left(D_2^i + D_3^i\right) \frac{\partial^2}{\partial x \partial y},$$

$$s_{2,3+I+i} = s_{3+I+i,2} = D_3^i \frac{\partial^2}{\partial x^2} + D_1^i \frac{\partial^2}{\partial y^2},$$

$$s_{33} = C_3^I \left(\frac{\partial^2}{\partial x^2} + \frac{\partial^2}{\partial y^2} \right), \quad s_{3,3+i} = -s_{3+i,3} = \alpha_3^i \frac{\partial}{\partial x},$$

$$s_{3,3+I+i} = -s_{3+I+i,3} = \alpha_3^i \frac{\partial}{\partial y},$$

$$s_{3+i,3+j} = \eta_{1ij} \frac{\partial^2}{\partial x^2} + \eta_{3ij} \frac{\partial^2}{\partial y^2} - \alpha_3^i \delta_{ij},$$

$$s_{3+i,3+I+j} = s_{3+I+j,3+i} = \left(\eta_{2ij} + \eta_{3ij}\right) \frac{\partial^2}{\partial x y},$$

$$s_{3+I+i,3+I+j} = \eta_{3ij} \frac{\partial^2}{\partial x^2} + \eta_{1ij} \frac{\partial^2}{\partial y^2} - \alpha_3^i \delta_{ij}, \quad i,j = \overline{1,I},$$

where

$$\alpha_1^i = \frac{E_i h_i}{1 - v_i^2}, \quad \alpha_2^i = \alpha_1^i v_i, \quad \alpha_3^i = \alpha_1^i \frac{1 - v_i}{2},$$

$$\beta_k^i = \alpha_k^i h_i, \quad \gamma_k^i = \beta_k^i h_i, \quad C_k^i = \sum_{j=1}^{i} \alpha_k^j, \quad D_k^i = \left(C_k^I - C_k^i\right) h_i + \frac{\beta_k^i}{2},$$

$$K_k^i = \left(C_k^I - C_k^i\right) h_i^2 + \frac{\gamma_k^i}{3}, \quad \eta_{kij} = \begin{cases} h_j D_k^i, & j < i \\ K_k^i, & j = i, \\ h_i D_k^j, & j > i \end{cases}$$

$$\delta_{ij} = \begin{cases} 1, & i = j \\ 0, & i \neq j \end{cases}, \quad i,j = \overline{1,I}, \quad k = 1,2,3.$$

Appendix B

$$b_{11}^1 = \left(C_1^I n_x^2 + C_2^I n_y^2\right) \frac{\partial}{\partial x} + 2C_3^I n_x n_y \frac{\partial}{\partial y},$$

$$b_{12}^1 = 2C_3^I n_x n_y \frac{\partial}{\partial x} + \left(C_2^I n_x^2 + C_1^I n_y^2\right) \frac{\partial}{\partial y}, \quad b_{13}^1 = 0,$$

$$b^1_{1,3+i} = \left(D^i_1 n_x^2 + D^i_2 n_y^2\right)\frac{\partial}{\partial x} + 2D^i_3 n_x n_y \frac{\partial}{\partial y},$$

$$b^1_{1,3+I+i} = 2D^i_3 n_x n_y \frac{\partial}{\partial x} + \left(D^i_2 n_x^2 + D^i_1 n_y^2\right)\frac{\partial}{\partial y},$$

$$b^1_{21} = \left(C^I_2 - C^I_1\right)n_x n_y \frac{\partial}{\partial x} + C^I_3\left(n_x^2 - n_y^2\right)\frac{\partial}{\partial y},$$

$$b^1_{22} = C^I_3\left(n_x^2 - n_y^2\right)\frac{\partial}{\partial x} - \left(C^I_2 - C^I_1\right)n_x n_y \frac{\partial}{\partial y}, \quad b^1_{23} = 0,$$

$$b^1_{2,3+i} = \left(D^i_2 - D^i_1\right)n_x n_y \frac{\partial}{\partial x} + D^i_3\left(n_x^2 - n_y^2\right)\frac{\partial}{\partial y},$$

$$b^1_{2,3+I+i} = D^i_3\left(n_x^2 - n_y^2\right)\frac{\partial}{\partial x} - \left(D^i_2 - D^i_1\right)n_x n_y \frac{\partial}{\partial y},$$

$$b^1_{31} = b^1_{32} = 0, \quad b^1_{33} = C^I_3\left(n_x \frac{\partial}{\partial x} + n_y \frac{\partial}{\partial y}\right),$$

$$b^1_{3,3+i} = \alpha^i_3 n_x, \quad b^1_{3,3+I+i} = \alpha^i_3 n_y,$$

$$b^1_{3+i,1} = b^1_{1,3+i}, \quad b^1_{3+i,2} = b^1_{1,3+I+i}, \quad b^1_{3+i,3} = 0,$$

$$b^1_{3+i,3+j} = \left(\eta_{1ij} n_x^2 + \eta_{2ij} n_y^2\right)\frac{\partial}{\partial x} + 2\eta_{3ij} n_x n_y \frac{\partial}{\partial y},$$

$$b^1_{3+i,3+I+j} = 2\eta_{3ij} n_x n_y \frac{\partial}{\partial x} + \left(\eta_{2ij} n_x^2 + \eta_{1ij} n_y^2\right)\frac{\partial}{\partial y},$$

$$b^1_{3+I+i,1} = b^1_{2,3+i}, \quad b^1_{3+I+i,2} = b^1_{2,3+I+i}, \quad b^1_{3+I+i,3} = 0,$$

$$b^1_{3+I+i,3+j} = \left(\eta_{2ij} - \eta_{1ij}\right)n_x n_y \frac{\partial}{\partial x} + \eta_{3ij}\left(n_x^2 - n_y^2\right)\frac{\partial}{\partial y},$$

$$b^1_{3+I+i,3+I+j} = \eta_{3ij}\left(n_x^2 - n_y^2\right)\frac{\partial}{\partial x} - \left(\eta_{2ij} - \eta_{1ij}\right)n_x n_y \frac{\partial}{\partial y},$$

$$b^2_{11} = n_x, \quad b^2_{12} = n_y, \quad b^2_{13} = b^2_{1,3+i} = b^2_{1,3+I+i} = 0,$$

$$b^2_{21} = -n_y, \quad b^2_{22} = n_x, \quad b^2_{23} = b^2_{2,3+i} = b^2_{2,3+I+i} = 0,$$

$$b^2_{31} = b^2_{32} = b^2_{3,3+i} = b^2_{3,3+I+i} = 0, \quad b^2_{33} = 1,$$

$$b^2_{3+i,1} = b^2_{3+i,2} = b^2_{3+i,3} = 0, \quad b^2_{3+i,3+j} = n_x,$$

$$b^2_{3+i,3+I+j} = n_y, \quad b^2_{3+I+i,1} = b^2_{3+I+i,2} = b^2_{3+I+i,3} = 0,$$

$$b^2_{3+I+i,3+j} = -n_y, \quad b^2_{3+I+i,3+I+j} = n_x, \quad i,j = \overline{1,I}.$$

Appendix C

$$\lambda^{mn}_{11} = C^I_1 \frac{m^2\pi^2}{A^2} + C^I_3 \frac{n^2\pi^2}{B^2}, \quad \lambda^{mn}_{12} = \lambda^{mn}_{21} = \left(C^I_2 + C^I_3\right) \frac{mn\pi^2}{AB},$$

$$\lambda^{mn}_{13} = \lambda^{mn}_{31} = 0, \quad \lambda^{mn}_{1,3+i} = \lambda^{mn}_{3+i,1} = D^i_1 \frac{m^2\pi^2}{A^2} + D^i_3 \frac{n^2\pi^2}{B^2},$$

$$\lambda^{mn}_{1,3+I+i} = \lambda^{mn}_{3+I+i,1} = \left(D^i_2 + D^i_3\right) \frac{mn\pi^2}{AB},$$

$$\lambda^{mn}_{22} = C^I_3 \frac{m^2\pi^2}{A^2} + C^I_1 \frac{n^2\pi^2}{B^2}, \quad \lambda^{mn}_{23} = \lambda^{mn}_{32} = 0,$$

$$\lambda^{mn}_{2,3+i} = \lambda^{mn}_{3+i,2} = \left(D^i_2 + D^i_3\right) \frac{mn\pi^2}{AB},$$

$$\lambda^{mn}_{2,3+I+i} = \lambda^{mn}_{3+I+i,2} = D^i_3 \frac{m^2\pi^2}{A^2} + D^i_1 \frac{n^2\pi^2}{B^2},$$

$$\lambda^{mn}_{33} = C^I_3 \left(\frac{m^2\pi^2}{A^2} + \frac{n^2\pi^2}{B^2} \right),$$

$$\lambda^{mn}_{3,3+i} = \lambda^{mn}_{3+i,3} = \alpha^i_3 \frac{m\pi}{A}, \quad \lambda^{mn}_{3,3+I+i} = \lambda^{mn}_{3+I+i,3} = \alpha^i_3 \frac{n\pi}{B},$$

$$\lambda^{mn}_{3+i,3+j} = \eta_{1ij} \frac{m^2\pi^2}{A^2} + \eta_{3ij} \frac{n^2\pi^2}{B^2} + \alpha^i_3 \delta_{ij},$$

$$\lambda^{mn}_{3+i,3+I+j} = \lambda^{mn}_{3+I+j,3+i} = \left(\eta_{2ij} + \eta_{3ij}\right) \frac{mn\pi^2}{AB},$$

$$\lambda^{mn}_{3+I+i,3+I+j} = \eta_{3ij} \frac{m^2\pi^2}{A^2} + \eta_{1ij} \frac{n^2\pi^2}{B^2} + \alpha^i_3 \delta_{ij}, \quad i,j = \overline{1,I}.$$

References

Altiero, N.J., Sikarskie, D.L., 1978. A boundary integral method applied to plates of arbitrary plan form. Comput. Struct. 9, 163–168.
Banerjee, P.K., Butterfield, R., 1981. Boundary Element Methods in Engineering Science. McGraw-Hill, New York.
Brebbia, C.A., Telles, J.C.F., Wrobel, L.C., 1984. Boundary Element Techniques Theory and Application in Engineering. Springer, Berlin.
Goloskokov, Ye.G., Filippov, A.P., 1977. Non-Stationary Vibrations of Deformable Systems. Naukova Dumka, Kiev.
Jaswon, M.A., Maiti, M., 1968. An integral formulation of plate bending problems. J. Engng. Math. 2, 83–93.

Rashed, Y.F., 1998. Boundary Element Formulations for Thick Plates. Computational Mechanics Publications, Billerica, MA.
Reddy, J.N., 1997. Mechanics of Laminated Composite Plates: Theory Analysis. CRC Press, Boca Raton, FL.
Shupikov, A.N., Smetankina, N.V., Sheludko, H.A., 1996. Minimization of the mass of multilayer plates at impulse loading. AIAA J. 34 (8), 1718–1724.
Segerlind, L.J., 1976. Applied Finite Element Analysis. Wiley, New York.
Smetankina, N.V., Sotrikhin, S.Yu., Shupikov, A.N., 1995. Theoretical and experimental investigation of vibration of multilayer plates under the action of impulse and impact loads. Int. J. Solids Struct. 32 (8/9), 1247–1258.
Zielinski, A.P., 1980. On curvilinear distribution expressed by double Fourier series. J. Appl. Math. Phys. 31, 717–729.
Zielinski, A.P., 1985. A contour series method applied to shells. Thin-Walled Struct. 3, 217–229.
Zienkiewicz, O.C., 1971. The Finite Element Method in Engineering Science. McGraw-Hill, London.